Ore Geology Reviews 65 (2015) 929–939

Contents lists available at ScienceDirect

Ore Geology Reviews

journal homepage: www.elsevier.com/locate/oregeorev

In-situ LA-ICP-MS trace elemental analyses of magnetite: Cu-(Au, Fe) deposits in the Khetri copper belt in Rajasthan Province, NW India

Wei Terry Chen [a,b], Mei-Fu Zhou [a,b,*], Xiaochun Li [b], Jian-Feng Gao [c], Kejun Hou [d]

[a] State Key Laboratory of Ore Deposit Geochemistry, Institute of Geochemistry, Chinese Academy of Sciences, Guiyang 550002, China
[b] Department of Earth Sciences, University of Hong Kong, Pokfulam Road, Hong Kong, China
[c] State Key Laboratory for Mineral Deposits Research, Nanjing University, Nanjing 210093, China
[d] Institute of Mineral Resources, Chinese Academy of Geological Sciences, Beijing 100037, China

ARTICLE INFO

Article history:
Received 29 July 2014
Received in revised form 23 September 2014
Accepted 29 September 2014
Available online 5 October 2014

Keywords:
Magnetite
Trace element composition
LA-ICP-MS
Khetri copper belt
NW India

ABSTRACT

Magnetite is common in many ore deposits and their host rocks, and is useful for petrogenetic studies. In the Khetri copper belt in Rajasthan Province, NW India, there are several Cu-(Au, Fe) deposits associated with extensive Cu ± Fe ± Au ± Ag ± Co ± REE ± U mineralization hosted in phyllites, schists and quartzites of the Paleoproterozoic Delhi Supergroup. Ore bodies of these deposits comprise dominantly disseminated and vein-type Cu-sulfide ores composed of chalcopyrite, pyrite, and pyrrhotite intergrown with minor magnetite. There are also Fe-oxide ores with minor or no Cu-sulfides, which are locally overprinted by the mineral assemblage of the Cu-sulfide ores. In addition to the Fe-oxide and Cu-sulfide ores, the protolith of the Delhi Supergroup includes banded iron formations (BIFs) with original magnetite preserved (i.e. magnetite-quartzites) and their sheared counterparts. In the sheared magnetite-quartzites, their magnetite and quartz are mobilized and redistributed to magnetite and quartz bands. Trace elemental compositions of magnetite from these types of ores/rocks were obtained by LA-ICP-MS. The dataset indicates that different types of magnetite have distinct concentrations of Ti, Al, Mg, Mn, V, Cr, Co, Ni, Zn, Cu, P, Ge and Ga, which are correlated to their forming environments. Magnetite grains in magnetite-quartzites have relatively high Al (800–8000 ppm), Ti (150–900 ppm) and V (300–600 ppm) contents compared to those of BIFs in other regions such as the Yilgarn Craton, Western Australia and Labrador, Canada. The high Al, Ti and V contents can be explained by precipitation of the magnetite from relatively reduced, Al–Ti-rich water possibly involving hotter, seafloor hydrothermal fluids derived from submarine mafic volcanic rocks. Magnetite in sheared magnetite-quartzites is generally irregular and recrystallized, and has Ni, Mn, Al, Cu and P contents lower than the magnetite from the unsheared counterparts, suggesting that the shearing-related mobilization is able to extract these elements from original magnetite. However, elevated contents of Ti, V, Co, Cr, Ge and Mg of the magnetite in the sheared magnetite-quartzites can be ascribed to involvement of external hydrothermal fluids during the shearing, consistent with occurrence of some hydrothermal minerals in the samples.

Compositions of magnetite from the Fe-oxide and Cu-sulfide ores are interpreted to be controlled mainly by fluid compositions and/or oxygen fugacity (fO_2). Other potential controlling factors such as temperature, fluid–rock interaction and co-precipitating minerals have very limited impacts. Magnetite in the Cu-sulfide ores has higher V but lower Ni contents than that of the Fe-oxide ores, likely indicating its precipitation from relatively reduced, evolved fluids. However, it is also indicated that the two types of magnetite do not show large distinctions in terms of concentrations of most elements, suggesting that they may have precipitated from a common, evolving fluid. We propose a combination of Ge versus Ti/Al and Cr versus Co/Ni co-variation plots to discriminate different types of magnetite from the Khetri copper belt. Our work agrees well with previous studies that compositions of magnetite can be potentially useful for provenance studies, but also highlights that discrimination schemes would be more meaningful for deposits in a certain region if fluid/water chemistry and specific formation conditions reflected in compositions of magnetite are clearly understood.

1. Introduction

Magnetite ($Fe^{2+}Fe^{3+}{}_2O_4$) is one of the most common oxide minerals of the spinel group. It occurs widely in various rocks, and can be a common ore mineral in many magmatic and hydrothermal deposits

* Corresponding author at: State Key Laboratory of Ore Deposit Geochemistry, Institute of Geochemistry, Chinese Academy of Sciences, Guiyang 550002, China.
E-mail address: mfzhou@hku.hk (M.-F. Zhou).

http://dx.doi.org/10.1016/j.oregeorev.2014.09.035
0169-1368/

and banded iron formations (BIFs) (e.g., Klein, 2005; Nadoll et al., 2012, 2014;Wager and Brown, 1968). It can form in a wide range of temperatures and is able to incorporate many trace elements (e.g., Mg, Al, Sc, Ti, V, Cr, Mn, Co, Ni, Zn, Ga, Ge, Y, Hf, Nb, Mo, Ta and Zr) in addition to Fe during its formation (Dare et al., 2012, 2014; Klemm et al., 1985; Lister, 1966; Nadoll and Koenig, 2011; Nadoll et al., 2012). The likelihood of the incorporation depends on many parameters mainly including the similarity of the ionic radii and the valence of the cations, oxygen fugacities, magma/fluid compositions, and temperature (Buddington and Lindsley, 1964; Dare et al., 2014; Frost and Lindsley, 1991; Goldschmidt, 1958; Nadoll et al., 2014 and references therein; Toplis and Carroll, 1995). As such, compositions of magnetite from a wide variety of deposit types have been the focus of many studies (e.g., Dupuis and Beaudoin, 2011 and references therein; Nadoll et al., 2012, 2014). In particular, recent development of laser ablation-inductively coupled plasma-mass spectrometry (LA-ICP-MS) allows in-situ measurement of a wide range of trace elements with detection limits below ppm (Liu et al., 2008; Nadoll and Koenig, 2011).

It has been suggested that some specific elements of magnetite can be used to discriminate magnetite from different geological settings (e.g., Dupuis and Beaudoin, 2011; Nadoll et al., 2014). Many studies have demonstrated that magmatic magnetite is extremely rich in both Ti and V (Dare et al., 2012; Liu et al., 2015-in this issue; Zhou et al., 2005, 2013), and thus enrichments of these two elements are commonly used to discriminate magmatic magnetite from low-temperature hydrothermal deposits or BIFs (e.g., Dupuis and Beaudoin, 2011; Nadoll et al., 2014). Moreover, it is also though that Ni/Co ratios are sufficient to discriminate magmatic and hydrothermal magnetite (Dare et al., 2014). However, these proposed discriminators do not seem feasible for discriminating low-temperature hydrothermal deposits or BIFs. For example, although Dupuis and Beaudoin (2011) and Nadoll et al. (2014) proposed some schemes to discriminate magnetite of different hydrothermal deposits and BIFs based on Ni/(Cr + Mn), Ca + Al + Mn (or Al + Mn) and Ti + V contents, recent studies indicated that hydrothermal magnetite in some skarn deposits plots in almost all the defined fields of the schemes (e.g., Hu et al., 2014; Zhao and Zhou, 2015-in this issue). Therefore, whether those elements or ratios can be used to discriminate magnetite from different hydrothermal deposits or BIFs, and how specific formation conditions are reflected in compositions of the hydrothermal magnetite still need rigorous examinations with more case studies.

The Khetri copper belt in Rajasthan Province, NW India has long been well-known for extensive Cu ± Au ± Fe mineralization (e.g., Knight et al., 2002). In this belt, magnetite is a common mineral in different ores and hosting rocks of the Cu-(Au, Fe) deposits, thus providing a good opportunity to understand how compositions of different types of magnetite are controlled by specific conditions or processes. Here we present in-situ LA-ICP-MS trace elemental data of magnetite from hosting magnetite-quartzites and their sheared counterparts nearby faults, Fe-oxide and Cu-sulfide ores in the Cu-(Au, Fe) deposits of the Khetri copper belt, Rajasthan Province, NW India. This new dataset is used to characterize different types of magnetite, aiming to ascertain whether compositions of the magnetite can be used to distinguish different formation processes. In addition, we explore possible application of trace element compositions of magnetite for provenance studies.

2. Geological background

2.1. Regional geology

The Aravalli mountain range is dominated by ca. 700 km long, NE-SW trending Precambrian rocks in Rajasthan Province, NW India (Fig. 1a). It constitutes a ~3.3–2.5 Ga basement complex, known as the Banded Gneissic Complex, composed of granitic gneisses and granites with minor units of meta-sedimentary and metavolcanic rocks (Gopalan et al., 1990; Roy and Kröner, 1996; Wiedenbeck and Goswami, 1994; Wiedenbeck et al., 1996). The basement complex is overlain by the ~2.2–1.85 Ga supracrustal sequences of the Aravalli and younger Delhi fold belts (Kaur et al., 2007, 2009, 2011). The sequences were suggested to deposit in continental rifting basins (e.g. Bhattacharya and Bull, 2010; Singh, 1988; Sinha-Roy, 1988). The NE-SW trending Delhi fold belt distributes in the northern and western parts of the Aravalli mountain range, and rocks of this fold belt are incorporated as the Delhi Supergroup. The supergroup in the northeastern terrane is divided into the Raialo, Alwar and Ajabgarh Groups from bottom upwards (e.g., Roy, 2000).

The Khetri copper belt in Rajasthan Province, NW India, extending for more than 200 km, is located in the north-westernmost part of the Aravalli mountain range (Fig. 1a). In this copper belt, Precambrian rocks are dominated by the ~1.85–1.70 Ga meta-sedimentary and volcanic sequence of the Delhi Supergroup (Biju-Sekhar et al., 2003; Kaur et al., 2007, 2009, 2011). The sequence in this region is subdivided into the Alwar and younger Ajabgarh Groups (Fig. 1b). The Alwar Group is composed mainly of metamorphosed mafic volcanic rocks, iron formation, conglomerate and sandstone, i.e. amphibolite, and feldspathic, magnetite and amphibole quartzites (Fig. 2a), whereas the Ajabgarh Group comprises metamorphosed stromatolitic carbonate, siltstone and shale, i.e. marble, phyllite, pelitic and garnet-chalorite-amphibole schists (Fig. 1c). Locally, the strata nearby faults are highly sheared in shear zones, characterized by obvious foliation or deformation (Fig. 2b). Both groups have a similar thickness of ca. 1300 m, and the contact between the two is gradational and conformable (Das Gupta, 1968; Sarkar and Dasgupta, 1980). These two groups are unconformably underlain by ~1820 Ma granitic intrusions, and were intruded by numerous granites with zircon U–Pb ages of 1720–1700 Ma (Kaur et al., 2007, 2011). The ~1820 Ma granitic intrusions have geochemical features similar to calc-alkaline magmatism, and were suggested to be subduction-related (Kaur et al., 2009). In contrast, the 1720–1700 Ma granites have affinity of rift-related, A-type granites (Chaudhri et al., 2003; Kaur et al., 2006, 2007, 2011).

2.2. Styles of mineralization in the Khetri copper belt

The Khetri copper belt covering an area of >200 km × 50 km contains more than 50 Cu-(Au, Fe) deposits and prospects associated with extensive Cu ± Au ± Fe ± Ag ± Co ± REE ± U mineralization hosted in the Paleoproterozoic meta-sedimentary and meta-volcanic rocks of the Alwar and Ajabgarh Groups. Large Cu-(Au, Fe) deposits are mostly distributed in the northeastern part of the copper belt, nearby the Khetri and Gothra Towns, including the Banwas, Madhan-Kudhan, Kalapaha, Kolihan, and Chandmari from northeast to southwest (Fig. 1c). It was estimated that the Madhan-Kudhan mine contains 66 Mt of ores with an average grade of 1.12–1.71% Cu, 0.2–0.6 g/t Au and 2–8 g/t Ag, whereas the Kolihan, Chandmari and Banwas mines have a total reserve of >70 Mt ores with an average grade of 1.14–1.7% Cu, 0.2–1 g/t Au and 2 g/t Ag (Knight et al., 2002).

In the Khetri-Gothra region, the mineralization is hosted mainly in garnet-chlorite-amphibole schists, andalusite- and graphite-bearing biotite schists, phyllites and amphibole- or feldspathic quartzites (Fig. 1d). The Cu-(Au, Fe) ore bodies occur as sub-vertical lens or irregular bodies (Fig. 1d), and are sited in sub-vertical NE- and NW-striking shear zones roughly along the contacts between the Alwar and Ajabgarh Groups. The ore bodies are broadly parallel to foliations in the host rocks, but also crosscut bedding and metamorphic fabrics (Fig. 1d). The Cu-(Au, Fe) ore bodies comprise dominantly massive, disseminated to vein-type Cu-sulfide ores composed of chalcopyrite, pyrite and pyrrhotite with minor magnetite (Fig. 2d). Other types of ores including the oxide-sulfide and Fe-oxide ores are minor and locally present in the Cu-(Au, Fe) ore bodies (e.g., Fig. 2c) (Knight et al., 2002). Oxide-sulfide ores are composed of sub-equal sulfides (chalcopyrite, pyrite or pyrrhotite) and Fe-oxide (magnetite and/or hematite), whereas Fe-oxide ores are dominated by magnetite and/or hematite without or with minor sulfides. It is noted that the sulfide-oxide ores are essentially Fe-oxide ores (as pods or disseminations) overprinted or crosscut by mineral

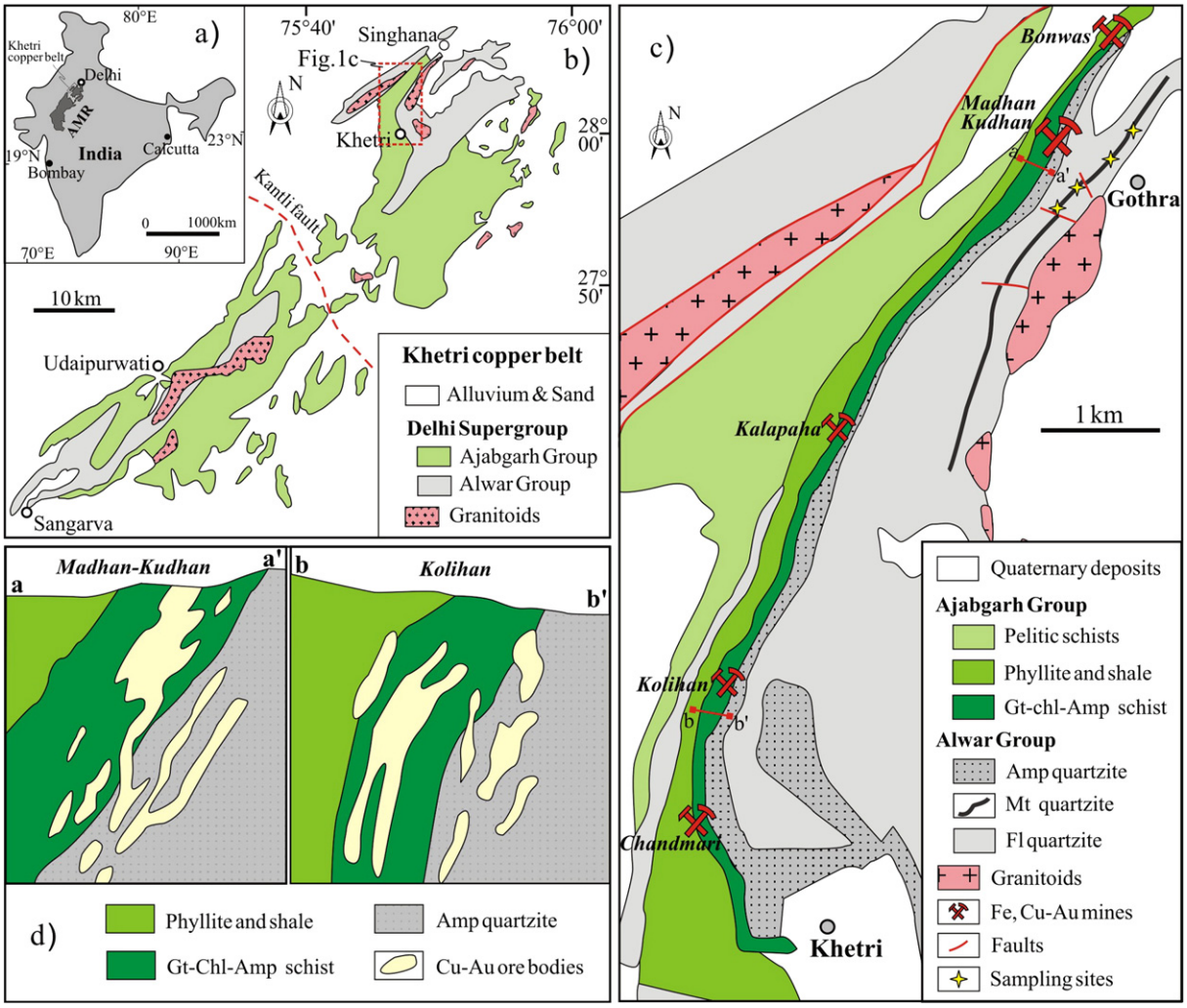

Fig. 1. a) Distribution of Aravalli mountain range (AMR) in NW India; b) Geological map of the Khetri copper belt; c) A simplified geological map of the Khetri-Gothra region showing distribution of Cu deposits; d) Cross-sections of the Madhan-Kudhan and Kolihan deposits showing the relationships between ore bodies and different host rocks. b) and c) are modified after Kaur and Mehta (2005), Kaur et al. (2006) and local geological report, respectively, while d) is modified after Knight et al. (2002). Also shown in c) are sampling sites of magnetite-quartzites.

assemblages of the Cu-sulfide ores (Fig. 2c). Therefore, the Cu-(Au, Fe) deposits in the Khetri copper belt have a paragenetic sequence of earlier Fe mineralization forming magnetite, albite, chlorite, amphibole and/or apatite, followed by Cu-(Au, Fe) mineralization forming chalcopyrite, pyrite, pyrrhotite, calcite, and quartz (Fig. 3c and d).

Alteration in the Khetri copper belts includes mainly early calc-silicate and late albite-hematite-magnetite alterations, overprinting the hosting metamorphic rocks (Knight et al., 2002). The calc-silicate alteration is characterized by an assemblage of pyroxene, actinolite, epidote, apatite, scapolite, titanite and magnetite, whereas albite-hematite-magnetite alteration is spatially related to Fe, Cu and Au mineralization, and characterized by an assemblage of albite, amphibole, magnetite, hematite, and calcite with variable amounts of biotite, scapolite, titanite, apatite, fluorite, chalcopyrite and pyrite. Knight et al. (2002) obtained a titanite U–Pb age of 847 ± 8 Ma for the regional alteration, and suggest that the epigenetic Cu-(Au, Fe) mineralization is broadly synchronous with 0.75–0.85 Ga A-type granites. Previous fluid inclusion studies indicated that fluids depositing early magnetite are high-temperature (540–560 °C) with low-salinity, whereas the Cu-(Au) mineralization is related to relatively highly saline but low-temperature (280–480 °C) fluids. Sulfur isotopic compositions of chalcopyrite and pyrrhotite are broadly overlapping granitoids, mafic rocks and evaporites in the Khetri belt (Rollinson, 1993). On the basis of the styles of mineralization and regional calc-silicate and Na–Fe alteration and structural features of different deposits in the Khetri belt, Knight et al. (2002) proposed firstly that these deposits are comparable to those of known iron-oxide copper gold (IOCG) deposits worldwide.

3. Sampling and petrography

In addition to the Fe-oxide and Cu-sulfide ores of Cu-(Au, Fe) ore bodies, hosting magnetite-quartzite layers in the Alwar Group and their highly sheared or mobilized counterparts nearby faults contain also abundant magnetite (Figs. 1c, 2b). Magnetite from these different types of ores and hosting rocks are selected for trace elemental analyses. Sampling sites of magnetite-quartzites are indicated in Fig. 1c, whereas those of the magnetite and Cu-sulfide ores are not shown in the figure because these ores were all sampled from underground tunnels in the Madhan-Kudhan and Kolihan deposits.

The magnetite-quartzites are generally banded and are locally weathered or oxidized to be reddish in color (Fig. 2a). They are composed mainly of intergrown anhedral magnetite (30–50%) and quartz (50–70%) (Fig. 3a). Sheared magnetite quartzites generally comprise magnetite-rich and quartz-rich bands with sharp and curved contacts (Fig. 2b), consistent with their formation from mobilization or redistribution of magnetite and quartz during shearing. The sheared magnetite-quartzites are composed dominantly of recrystallized subhedral to anhedral magnetite and quartz with minor amounts of

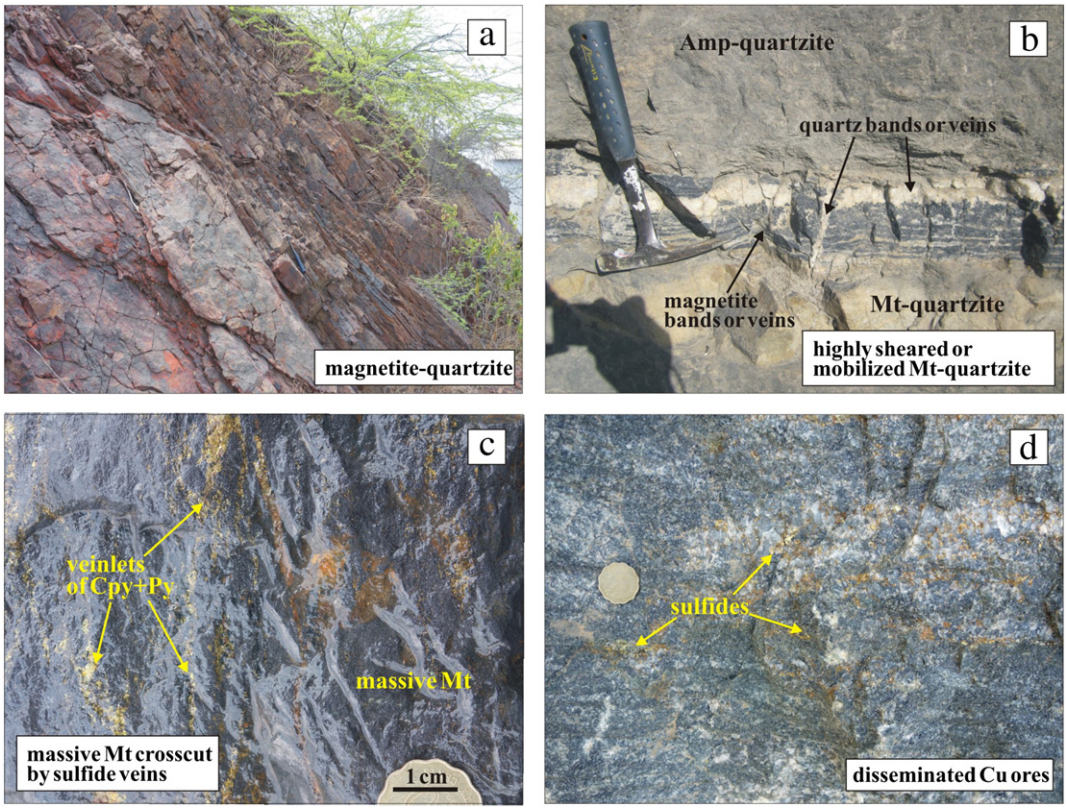

Fig. 2. Field photos of various hosting rocks and ores from different deposits in the Khetri copper belt. a) Magnetite-quartzite layers in the Alwar Group. Note that the layers are weathered or oxidized to be reddish in color; b) Highly sheared or mobilized magnetite-quartzites. Both magnetite and quartz are re-distributed to be bands or veins during shearing; c) Oxide-sulfide ores. Note that the massive magnetite ore is crosscut or overprinted by veinlets of chalcopyrite and pyrite; d) Disseminated Cu ore. Note that disseminated chalcopyrite distributes in quartzites, which is associated with alteration of calcite, albite, biotite and quartz. Abbreviations: Cpy—chalcopyrite; Mt—magnetite; Py—pyrite.

hydrothermal minerals including calcite, apatite and biotite (Fig. 3b). Fe-oxide ores sampled are massive and composed mainly of subhedral to anhedral magnetite with minor apatite, amphibole and albite (Fig. 3c). Cu-sulfide ores sampled are disseminated and vein-type (Fig. 2c, d), composed of chalcopyrite, pyrite, pyrrhotite, chlorite, quartz, calcite, and scapolite (Fig. 3d). Magnetite grains in Cu-sulfide ores are generally minor (<5 vol.%), and are mostly anhedral, occurring either as grains enclosed by chalcopyrite or intergrown with sulfides or other hydrothermal minerals. These magnetite grains may be synchronous with or slightly earlier than sulfides in the Cu-(Au) mineralization stage.

4. Analytical methods

Trace elements of magnetite were determined by a New Wave UP 213 Nd:YAG Laser Ablation system coupled with a Bruker Aurora M90 ICP-MS at the MRL Key Laboratory of Metallogeny and Mineral Assessment, Institute of Mineral Resources, Chinese Academy of Geological Sciences, Beijing, China. Detailed operating conditions for the laser ablation system and the ICP-MS instrument and data reduction have been described by Hou et al. (2009) and Gao et al. (2013). Helium was applied as a carrier gas, while argon was used as makeup gas and mixed with the helium via a T-connector before entering the ICP. Each analysis was performed by a laser spot of 40 μm in diameter with successive pulses at 10 Hz. Each analysis includes a background acquisition of approximately 20 s for gas blank, followed by data acquisition of 40 s from the sample. Element contents were calibrated against multiple reference materials (GSE-1G, BCR-2G, BIR-1G) using ^{57}Fe as the internal standard (Gao et al., 2013). Every ten analyses of samples were followed by one analysis of GSE-1G, BCR-2G and BIR-1G for quality control to correct the time-dependent drift of sensitivity and mass discrimination. Offline data reduction was performed on a soft ICPMSDataCal (Liu et al., 2008), including integration selection of background and analysis signals, and time drift correction and quantitative calibration. Trace elemental concentrations of all the magnetite and standards are provided in Appendix I.

5. Analytical results

5.1. Magnetite in magnetite-quartzites

Magnetite from magnetite-quartzites contains substantial Mg, Al, Si, Ca, Ti, Mn, V, Cr, Co, Ni, Cu, and Ga (Appendix I). Concentrations of other elements, e.g., Sc, Zn, Ge, Mo, Zr, and Pb, are either close to or below detection limits (Appendix I). These magnetite grains have large ranges of Al (~800–8000 ppm), Ti (~250–1600 ppm), Mn (20–750 ppm), Cr (1–100 ppm) and V (~250–650 ppm) (Appendix I; Fig. 4). In general, there are positive correlations between Ti and Al, Zn and Mn, and Cr and Ti (Fig. 4a, d, e), but negative correlation between Ga and V (Fig. 4b).

In order to compare different types of magnetite, the trace element concentrations are normalized to average compositions of all magnetite grains analyzed in this study. As shown in Fig. 5a, the magnetite from magnetite-quartzites is extremely depleted in Cr with a sample slightly enriched in Mn compared to the average values.

5.2. Magnetite in highly sheared magnetite-quartzites

Magnetite grains from highly sheared magnetite-quartzites have compositions different from those in the unsheared magnetite-quartzites (Figs. 4–6). They have concentrations of Ti (300–1600 ppm), V (600–1000 ppm), Ga (20–100 ppm), Cr (40–200 ppm), Ge (4–11 ppm) and Co (25–40 ppm) higher but concentrations of Al (400–3000 ppm), Ni (20–60 ppm), P (~0.01–400 ppm) and Cu (0.1–2 ppm) lower than the unsheared magnetite (Fig. 4). There are positive correlations between

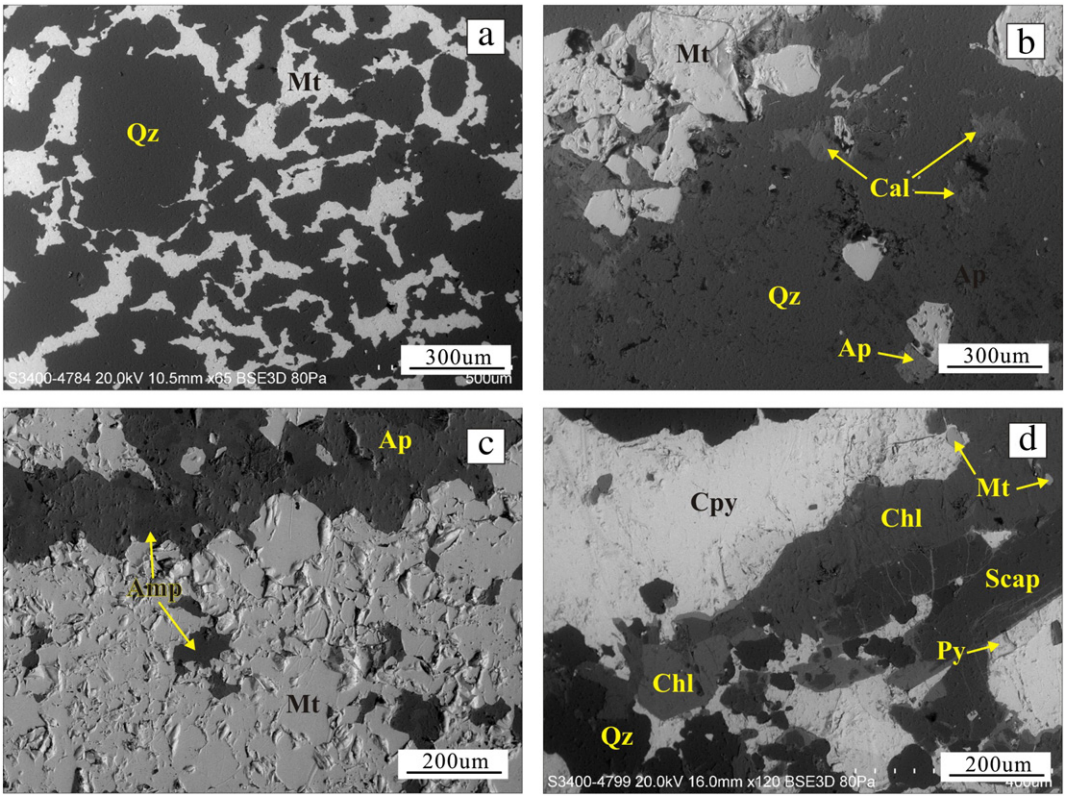

Fig. 3. Photomicrographs of different hosting rocks and ores in the Khetri copper belt. a) Magnetite-quartzite composed dominantly of intergrown anhedral magnetite and quartz. BSE photo; b) Highly sheared or mobilized quartzites composed mainly of recrystallized quartz and magnetite with minor calcite and apatite. BSE; c) Magnetite ore composed mainly of magnetite with minor and variable amounts of apatite and amphibolite. BSE; d) Cu-sulfide ore composed of chalcopyrite, pyrite, quartz, scapolite, chlorite with minor magnetite. BSE; d) Massive magnetite ore in the Dahongshan deposit. Mineral abbreviations: Mt—magnetite; Cal—calcite; Cpy—chalcopyrite; Py—pyrite; Ap—apatite; Chl—chlorite; Amp—amphibole; Scap—scapolite.

Al and Ti for the magnetite in the sheared magnetite-quartzites, but the trend of the correlation has a slope gentler than that of the unsheared magnetite (Fig. 4a). The compositional differences of both types of magnetite are also reflected in the multi-element diagram (Fig. 5b).

5.3. Magnetite in Fe-oxide ores

Magnetite grains from Fe-oxide ores exhibit limited variations in terms of trace elemental concentrations (Fig. 4). They have Al (800–2400 ppm), Ti (300–1000 ppm), Zn (7–10 ppm), Ge (7–10 ppm), Mg (80–800 ppm) and Mn (120–180 ppm) roughly overlapping with the magnetite in sheared magnetite-quartzites (Fig. 4), but have relatively low Cr (3–20 ppm), V (45–55 ppm), Ga (20–30 ppm) and Co (15–25 ppm) (Fig. 4). In the multi-element diagram, they have patterns characterized by extremely depleted V and Cr when compared to the magnetite in magnetite-quartzites and sheared counterparts (Fig. 5c).

5.4. Magnetite in Cu-sulfide ores

In general, except for the distinctly higher V (650–1100 ppm), Co (25–40), and Cr (850–2200 ppm) but lower Ni (20–60 ppm) (Fig. 4b, c, e), magnetite in Cu-sulfide ores has concentrations of many elements undistinguishable to the magnetite in the Fe-oxide ores (Fig. 4). On the other hand, they have much higher Cr and V but lower Ni than magnetite from the sheared magnetite-quartzites (Figs. 4 and 5c). In the multi-element diagram, the magnetite in Cu-sulfide ores has patterns characterized by relatively enriched V and Cr, but for the patterns of other elements, magnetite of Cu-sulfide ores is undistinguishable from those in Fe-oxide ores (Fig. 5c).

6. Discussion

6.1. Nature of different types of magnetite in the Khetri copper belt

Magnetite-quartzite layers of the Alwar Group in the Khetri belt are composed mainly of magnetite and quartz (Fig. 3a), similar to many metamorphosed BIFs worldwide. Also, the magnetite-quartzites sampled in this study do not show obvious deformation or foliation but only recrystallization. This is well indicated by the homogeneous distribution of magnetite and quartz in our samples (e.g., Fig. 3a). Because recrystallization process cannot significantly modify the compositions of original magnetite through subsolidus chemical redistribution due to simple mineralogy (e.g., only quartz), we consider that magnetite in the magnetite-quartzites is similar to originally BIF-type magnetite in terms of compositions. We thus term this type of magnetite as 'metamorphic BIF-type magnetite'. In contrast, the highly sheared or mobilized magnetite-quartzites sampled in this study are extensively foliated or modified by shearing (up to low-amphibolite facies; Gangopadhyay and Sen, 1967), resulting in recrystallization of magnetite and quartz and their re-distributions as veins or bands (Fig. 2b). The sheared magnetite-quartzites contain also minor hydrothermal minerals such as calcite and biotite, suggesting possible modification of the original metamorphic BIF-type magnetite by hydrothermal fluids during shearing.

Different from the metamorphic BIF-type magnetite and its mobilized counterparts, magnetite grains from the Fe-oxide and Cu-sulfide ores have crystallized from hydrothermal fluids, consistent with their occurrences in hydrothermal veins or replacing bodies associated with extensive alteration (Knight et al., 2002). Indeed, the close association of magnetite with hydrothermal minerals such as apatite, amphibole, quartz, biotite, scapolite and calcite in these ores (Fig. 3c, d) further

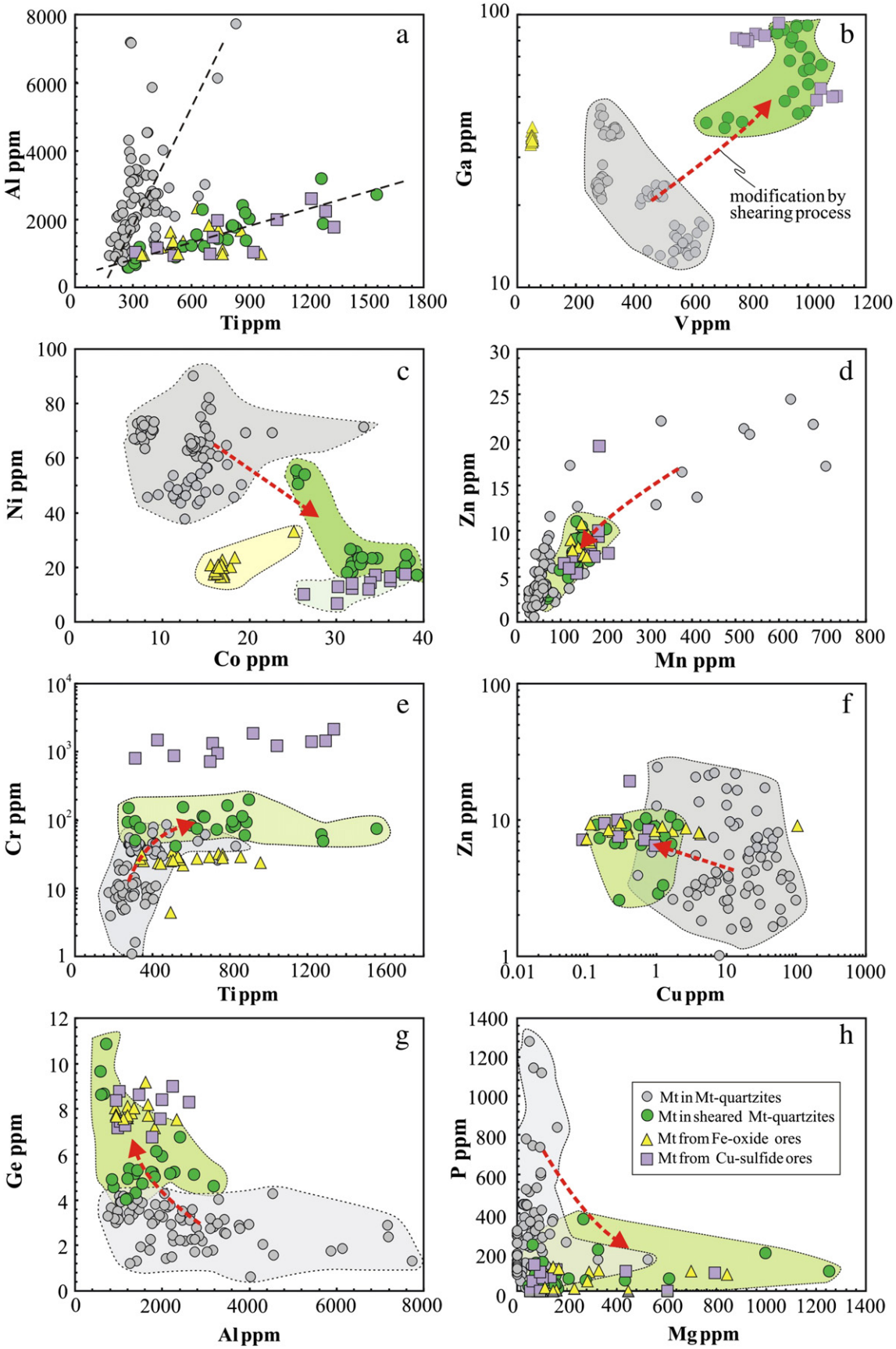

Fig. 4. Bi-modal plots of Ti vs. Al, V vs. Ga, Ni vs. Co, Zn vs. Mn, Ti vs. Cr, Zn vs. Cu, Ge vs. Al, and Mg vs. P in magnetite from different hosting rocks and ores in Khetri belt.

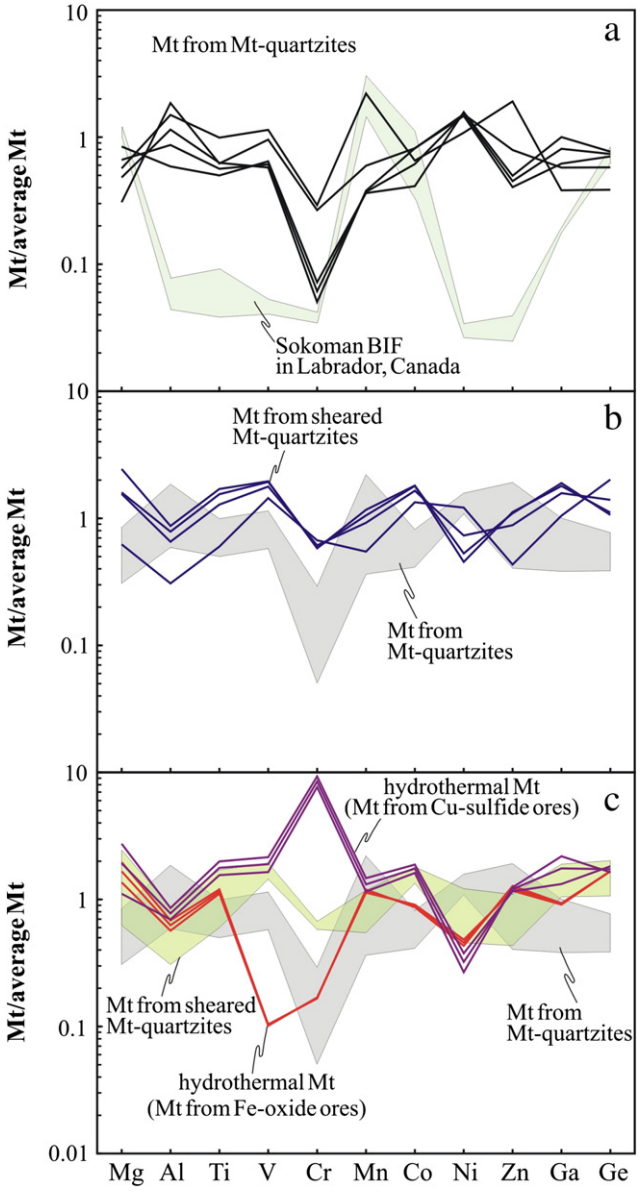

Fig. 5. Normalized multi-elemental patterns of magnetite from magnetite-quartzites (a), sheared magnetite-quartzites (b), barren magnetite and Cu-sulfide ores (c). Normalized values are the average composition of all the magnetite grains from hosting rocks and ores in the copper belt. Also shown in (a) is the pattern of magnetite from Sokoman iron formations in Labrador, Canada (Chung et al., 2015-in this issue).

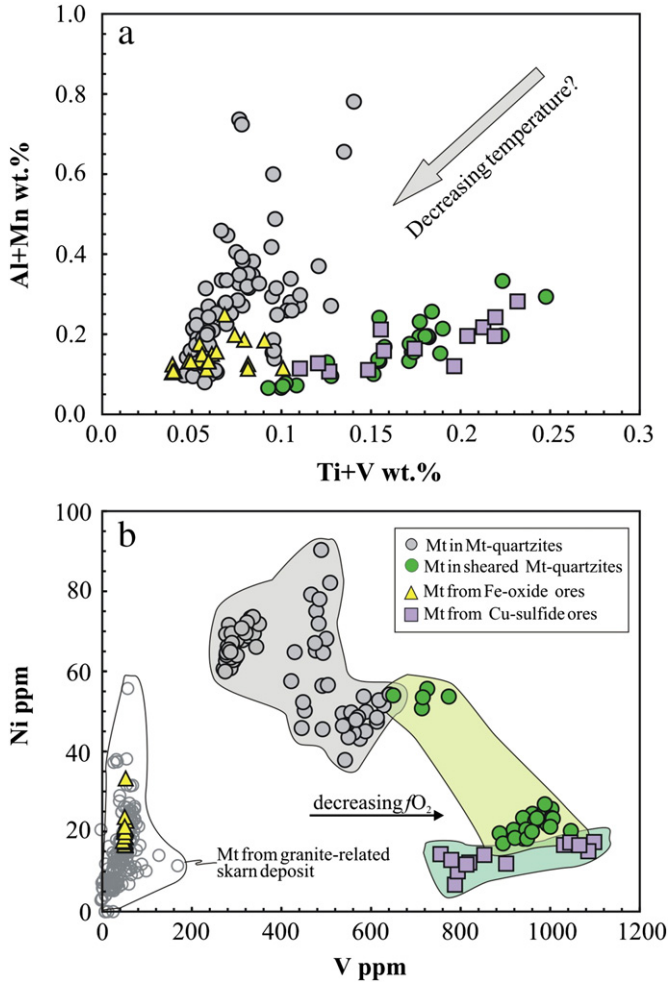

Fig. 6. Plots of Ni vs. V and Al + Mn vs. Ti + V showing the origin of magnetite from different hosting rocks and ores. Also plotted are the compositions of magnetite from the Tengtie granite-related Skarn-type deposit, SE China. It is noted that magnetite from barren magnetite ores has the lowest V, whereas that from Cu-sulfide ores has the highest V.

suggests that magnetite grains in the two types of ores precipitated from hydrothermal fluids. Currently, it is not clear that whether the magnetite and Cu-rich ores have formed from a common hydrothermal fluid system, because the magnetite ores are only locally present (Knight et al., 2002). Nevertheless, it is clear that early magnetite pods or patches are overprinted or crosscut by veins or bands of Cu-sulfides in oxide-sulfide ores, indicating that the Fe-oxide ores predate the Cu mineralization of the Cu-(Au, Fe) deposits in the Khetri copper belt.

6.2. Controlling factors and processes for variable magnetite compositions

Magnetite from different types of deposits can accommodate various trace elements depending on fluid/water/melt compositions and processes of magnetite precipitation (e.g., Dare et al., 2014; Frietsch and Perdahl, 1995; Nadoll et al., 2014; Nystrom and Henriquez, 1994; Toplis and Corgne, 2002). It has been demonstrated that composition of magmatic magnetite was mainly controlled by: 1) magma composition, 2) temperature (T), 3) pressure (P), 4) cooling rate, 5) oxygen or sulfur fugacity, and 6) silica activity (Nadoll et al., 2014 and references therein). However, it is not clear whether these factors are also available for magnetite formed in sedimentary, metamorphism and hydrothermal processes or conditions. For example, Carew (2004) pointed out that in addition to fluid compositions, P, T and fO_2, compositions of hosting rocks or coexisting minerals are also responsible for variable compositions of hydrothermal magnetite in different settings. In this section, we explore possible controlling factors for compositions of magnetite formed by different processes in the Khetri copper belt.

6.2.1. Metamorphic BIF-type magnetite

The BIF-type magnetite grains in the magnetite-quartzites show geochemical signatures quite different from other types of magnetite in Cu-(Au, Fe) deposits in the Khetri belt (e.g., Fig. 4), e.g., they have relatively low Cr, Ga and Ge but high Ni, P and Cu contents compared to the mobilized (or sheared) and hydrothermal magnetite (Fig. 4). Because the BIF-type magnetite has formed from chemical sedimentation from seawater, their variable compositions are likely controlled mainly by water compositions, and/or temperature and fO_2 (Nadoll et al., 2014). Compared to magnetite in other banded iron formations such as those in the Yilgarn Craton, Western Australia (Al = 0.27–1510 ppm; Ti = 0.8–117 ppm; V = 0.26–40.5 ppm; Nadoll et al., 2014) and Sokoman iron formation in Labrador, Canada (Fig. 5a) (Chung et al., 2015-in this issue), the metamorphic BIF-type magnetite in the Khetri belt has

dramatically high concentrations of Al (800–8000 ppm), Ti (150–900 ppm) and V (300–600 ppm). The fO_2 may control the V content because V with variable valence states (e.g., +3, +4 and +5) was suggested to be preferably enriched in more reduced fluids/water/melts (e.g., Toplis and Corgne, 2002). Therefore, it is likely that the higher V contents of the BIF-type magnetite than those in iron formations of Yilgarn and Labrador would be related to relatively reduced water with higher V concentrations. On the other hand, the relatively high Al and Ti contents of BIF-type magnetite may be indicative of high formation temperatures (c.f., Nadoll et al., 2014). However, it is noted that these BIF-type magnetite grains have Al contents even higher than magnetite in different ores in the Khetri belt with formation temperatures up to 500 °C (Fig. 4a), suggesting that temperature may not be a major or solely controlling factor. Another explanation is that the original BIF-type magnetite grains have precipitated from extremely Al–Ti-rich water compared to those in Yilgarn and Labrador. There is a common consensus that the formation of most BIFs has involved submarine volcano-derived hydrothermal fluids (e.g., Lascelles, 2007; Wang et al., 2014), and thus the high Al, Ti and even Ni contents of the originally BIF-type magnetite in the Khetri belt may be related to hydrothermal fluids derived from relatively mafic submarine volcanic rocks (c.f., Carew, 2004). Such a conclusion is also supported by the association of the magnetite-quartzites with mafic volcanic layers (now amphibolite) in the Delhi Supergroup.

6.2.2. Modification of magnetite by shearing process

The magnetite in sheared magnetite-quartzites in the Khetri belt formed from the original BIF-type magnetite through shearing process associated with mineral mobilization and recrystallization (Figs. 2b, 3b). In the bi-elemental plots for both the mobilized and original magnetite, it is clearly shown that concentrations of almost all elements of the original magnetite were changed during the shearing process (Fig. 4). Such compositional differences suggest that the shearing process is able to extract Ni, Mn, Al, Cu and P from the original magnetite (Fig. 4). However, it is also noted that Ti, V, Co, Cr, Ge and Mg of the mobilized magnetite are dramatically higher than those of the original magnetite, suggesting that these elements should be gained from external sources, either from the coexisting minerals or hydrothermal fluids as indicated by the presence of minor hydrothermal calcite, biotite and apatite in the sheared magnetite-quartzites (Fig. 3b). Coexisting minerals are mainly quartz that has extremely low Ti, V, Co, Cr, Ge and Mg, and would not provide these elements during mobilization or recrystallization involved in the shearing process. An alternative explanation is that the mobilized or recrystallized magnetite acquired these elements from external hydrothermal fluids likely channeled by the shear zone.

6.2.3. Magnetite precipitating from hydrothermal fluids

In the bi-modal plot of Al versus Ti, magnetite grains of the Fe-oxide and Cu-sulfides ores of Cu-(Au, Fe) deposits in the Khetri belt plot together along a correlation trend different from that of the metamorphic BIF-type magnetite in magnetite-quartzites (Fig. 4a), consistent with their distinct origins. Similarly, the mobilized magnetite in the shearing magnetite-quartzites whose formation involved external hydrothermal fluids also plots along the same trend for the magnetite in different ores (Fig. 4a). These similarities suggest that the formation of the magnetite in sheared magnetite-quartzites and ores may have involved a similar fluid system related to the Fe–Cu–Au mineralization of the Khetri copper belt. Such a conclusion is also supported by their comparable concentrations of most elements, such as Mn, Zn, Cu, Mg, P and Ge (Fig. 4). On the other hand, different concentrations of some other elements (e.g., Co, V, Cr, Ni) for magnetite from these two types of ores (Figs. 4 and 5c) may be ascribed to different degrees of evolution, fluid–rock interaction or co-precipitating minerals (Carew, 2004; Nadoll et al., 2014), as will be discussed below.

Composition of magnetite from the Fe-oxide and Cu-sulfide ores may be affected by chemical compositions of hosting rocks through fluid–rock interaction. Because the Cu-sulfide ores sampled are hosted in quartzites composed dominantly of quartz, such an effect of hosting rocks should be very limited. On the other hand, the magnetite ores are hosted in garnet-chlorite-amphibole schists and phyllites composed of variable silicate minerals. It seems that a variety of the silicate hosting rocks would have significant controls on compositions of magnetite in the magnetite ores. If the hosting rocks do have effects on the composition of magnetite in Fe-oxide ores, the magnetite should exhibit a large compositional variation, and also may have relatively high Ti, Ni, Co, Cr, or V compared to those hosted in quartzites, because some hosting schists (e.g., mafic volcanic rocks; Kaur and Mehta, 2005) are enriched in these elements (particularly Ti, V, or Cr). However, as shown in Fig. 4, concentrations of these elements are much lower than or similar to those in magnetite of the Cu-sulfide ores (Fig. 4b, c, e), indicative of limited effects of hosting rocks and fluid–rock interaction on compositions of magnetite.

Minerals co-precipitating with magnetite might also affect compositions of some specific trace elements of the magnetite due to different partition coefficients, such as sulfides preferably partitioning chalcophile elements (Ni, Co, Cu and Zn). The Fe-oxide ores are composed mainly of magnetite with minor and variable amounts of quartz, albite, calcite and apatite but without sulfides (Fig. 3c). Because V, Cr and Ti are highly partitioning into magnetite compared to the quartz, albite, calcite and apatite in the Fe-oxide ores (Neilson, 2003), their concentrations in magnetite cannot be principally affected by these minerals. On the other hand, the Cu-sulfide ores have an association of magnetite (<5 vol.%) and abundant sulfides (Fig. 3d). As Ni, Co, Cu and Zn would strongly partition into pyrite and chalcopyrite, magnetite in the Cu-sulfide ores may be relatively depleted in these elements when compared to that in the Fe-oxide ores, if both types of ores precipitated from a common, evolving fluid system. However, such a depletion is not expected (Fig. 4c, d, f), e.g., magnetite in the Cu-sulfide ores has Co and lower Ni contents higher than but Cu and Zn contents similar to that in the Fe-oxide ores (Fig. 4c, d, f). A possible explanation is that the magnetite in the Cu-(Au, Fe) mineralization stage crystallized synchronous with or slightly earlier than sulfides. This conclusion is also supported by the fact that some magnetite grains are enclosed in sulfides (Fig. 3d).

Both temperature and fO_2 may have influences on partition coefficients of some elements and thus their concentrations in magnetite (e.g., Ilton and Eugster, 1989; Toplis and Corgne, 2002). Experiments of Ilton and Eugster (1989) indicate that Cu, Zn and Mn tend to concentrate into lower-temperature hydrothermal fluids from which Cu, Zn and Mn-rich magnetite precipitated. Previous studies of fluid inclusions on the Cu-(Au, Fe) deposits showed that the formation temperatures for Fe-oxide and Cu-sulfide ores were 540–560 °C and 280–480 °C, respectively (Jaireth, 1984; c.f. Knight et al., 2002). As such, the Cu-(Au, Fe) mineralizing fluids would be expected to be enriched in Cu, Zn and Mn. However, magnetite from both Fe-oxide and Cu ores does not exhibit a large difference in terms of Cu, Zn and Mn contents (Fig. 4d, f), excluding a significant influence of temperature on concentrations of these elements in magnetite. Nadoll et al. (2014) identified that both Al + Mn and Ti + V contents in magnetite were positively correlated with formation temperatures for different hydrothermal deposits they summarized, and indicated that Al + Mn and Ti + V contents may increase with elevated temperatures. We also summarize our data of all types of magnetite from Cu-(Au, Fe) deposits in the Khetri belt, but do not find the expected trend in the plots of Al + Mn versus Ti + V (Fig. 6a). Even for the magnetite grains in Fe-oxide ores forming at highest temperatures, they have Al + Mn and Ti + V contents much lower than those in the Cu-sulfide ores. We thus conclude that the temperature is not a major responsibility for the compositional variability of these types of magnetite. However, it is noted that positive correlations between Ti + V and Al + Mn are still clear for each type of magnetite (Fig. 6a). We speculate that the temperature factor may just work

only on a single system or specific deposit, because such correlations are more likely related to differentiation of fluids/water. Oxygen fugacity (c) may control the concentration of V in magnetite (Toplis and Corgne, 2002), and thus the extremely low V concentration of the grains in Fe-oxide ores (Fig. 6b) may suggest that they have formed from relatively oxidized fluids compared to magnetite in Cu-sulfide ores, similar to the magnetite from the Tengtie granite-related skarn Fe deposit in South China (Zhao and Zhou, 2015-in this issue).

6.3. Magnetite as a discriminator for ore deposit types

Many researchers have proposed a number of discrimination diagrams to identify magnetite formed from different ore-forming environments, or different types of ore deposits (Carranza et al., 2012; Dare et al., 2014; Dupuis and Beaudoin, 2011; Nadoll et al., 2012, 2014; Pearce and Gale, 1977). Our new findings of this study on geochemistry of different types of magnetite from the Cu-(Au, Fe) deposits of the Khetri copper belt agree well with these previous studies that magnetite forming at different environments can be different in terms of trace elemental compositions and thus useful for provenance studies.

Nickel, Cr, Si, Mg, Ca, Ti, V and Mn in magnetite were suggested to be very good indicators for distinguishing mineral deposit types including IOCG, Kiruna, BIFs, porphyry Cu–Au, Fe–Cu skarn, magmatic Fe–Ti–V–Cr or Ni–Cu–PGE, and volcanogenic massive sulfide (VMS) (e.g., Dare et al., 2014; Dupuis and Beaudoin, 2011; Nadoll et al., 2014; Singoyi et al., 2006). Some researchers proposed some schemes to discriminate different types of deposits, such as the Ca + Mn + Al versus Ti + V and Ni/(Cr + Mn) versus Ti + V diagrams of Dupuis and Beaudoin (2011) and Ni/Co-Ti diagram of Dare et al. (2014). These diagrams do sufficiently discriminate the magmatic deposits from hydrothermal or sedimentary magnetite deposit due to the extremely high Ti, Al and V contents but low Ni/Cr ratios of the igneous magnetite. However, recent studies indicated that the defined schemes seem to be not always reliable for different types of magnetite from low-temperature hydrothermal deposits or BIFs (e.g., Huang et al., 2013; Hu et al., 2014; Zhao and Zhou, 2015-in this issue). Similarly, our new dataset in current study show that the BIF-type magnetite is clustered mainly in the 'IOCG' and 'Skarn' fields of the Ni/(Cr + Mn) versus Ti + V diagram, whereas magnetite from sheared magnetite-quartzites and different ores is plotted mostly in the 'Skarn' field (Fig. 7a). Also, in the Ca + Al + Mn versus Ti + V diagram the BIF-type magnetite does not plot in the expected 'BIF' field (Fig. 7b). These inconsistencies seem to indicate that these proposed schemes are insufficient to discriminate different types of hydrothermal deposits or BIFs from different regions. We consider that any proposed schemes should be only meaningful for discriminating deposits or rocks in a certain region if a detailed description of mineralogy and textural relationship (e.g., Nadoll et al., 2014) and the chemistry of the fluids/water from which the magnetite precipitate are clearly understood.

On the basis of our current compositional data, we propose some parameters or plots to discriminate these types of magnetite in the Cu-(Au, Fe) deposits in the Khetri copper belt (Fig. 8). Such discrimination diagrams should be useful for future provenance studies particularly on sedimentary rocks in the Khetri region, and may also shed light on further geochemical studies on magnetite from other region. We choose Ti/Al, Ge, Cr and Co/Ni for plotting, because these elements or ratios are dramatically different in different types of magnetite in the region. In the proposed plot of Ti/Al versus Ge, the BIF-type magnetite plotted away from the magnetite from the sheared magnetite-quartzites and different ores (Fig. 8a). Moreover, plot of Cr versus Co/Ni can sufficiently discriminate magnetite from different hosting rocks or ores in the belt, without any compositional overlaps (Fig. 8b). This discrimination scheme may be also plausible for hydrothermal deposits and BIFs in other regions because both Cr contents and Co/Ni ratios are principally related to fluids derived from variable magmas (Carew, 2004; Dare et al., 2014). For example, the fluids for the Fe-oxide and Cu-sulfide ores of the Cu-(Au, Fe) deposits in the Khetri belt were suggested to

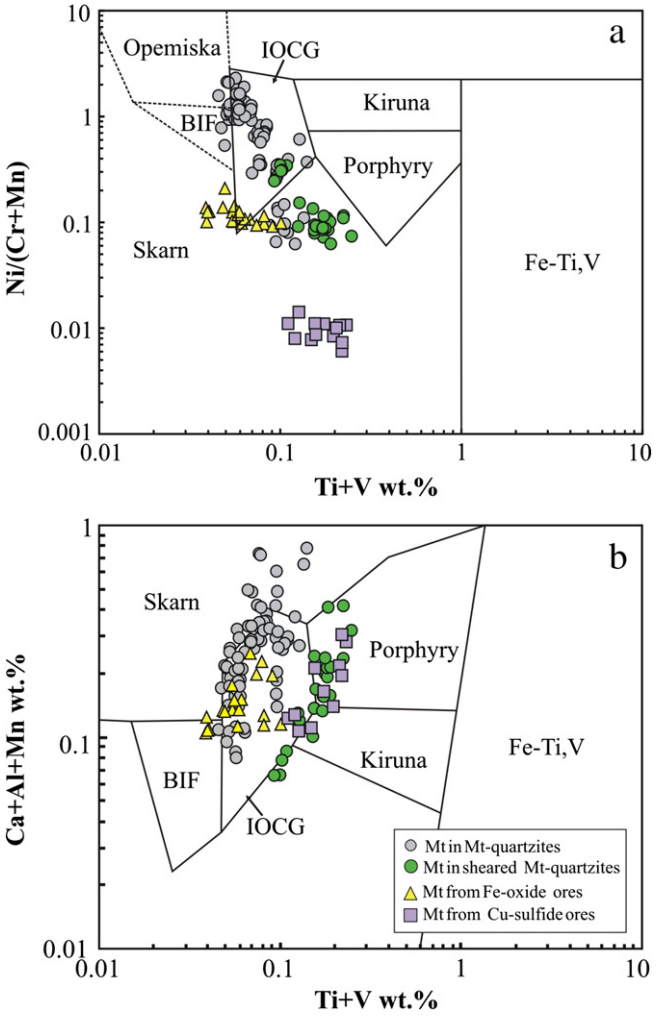

Fig. 7. Plots of V + Ti vs. Ca + Al + Mn and Ti + V vs. Ni/(Cr + Mn) of magnetite from hosting rocks and ores. Reference fields are after Dupuis and Beaudoin (2011). Noted that the sedimentary magnetite from quartzites plot mostly on 'IOCG' field. BIF: banded iron formation; Skarn: Fe–Cu skarn deposits; IOCG: iron-oxide-copper-gold deposits; Porphyry: porphyry Cu deposits; Kiruna: Kiruna apatite-magnetite deposits; Fe–Ti, V: magmatic Fe–Ti-oxide deposits.

be of a magmatic-hydrothermal origin (Jaireth, 1986), and the different Cr and Ni contents of magnetite from different ores may be related to different degrees of evolution of fluids or different nature of the magmas producing the fluids (e.g., mafic rocks or granitoids; Knight et al., 2002; Rollinson, 1993).

7. Conclusions

Magnetite in ores and country rocks from the Cu-(Au, Fe) deposits in the Khetri copper belt, Rajasthan Province, NW India, has variable and distinct concentrations of Ti, Al, Mg, Mn, V, Cr, Co, Ni, Zn, Cu, P, Ge and Ga, which can be correlated to the forming environments. Magnetite grains in magnetite-quartzites of original banded iron formation have different compositions with relatively low Ga and Ge but high Ni, P and Cu contents compared to hydrothermal magnetite grains. Shearing may mobilize Ni, P, Cu, Al and Mn from the original BIF-type magnetite, but elevated Ti, V, Co, Cr, Ge and Mg contents of the recrystallized magnetite are due to modification of external hydrothermal fluids possibly channeled along faults. Compositions of magnetite from Fe-oxide and Cu-sulfide ores are interpreted to be mainly controlled by fluid compositions and/or oxygen fugacity. Other potential factors including temperature, fluid–rock interaction and co-precipitating mineral phases play very limited roles on controlling composition of magnetite. A

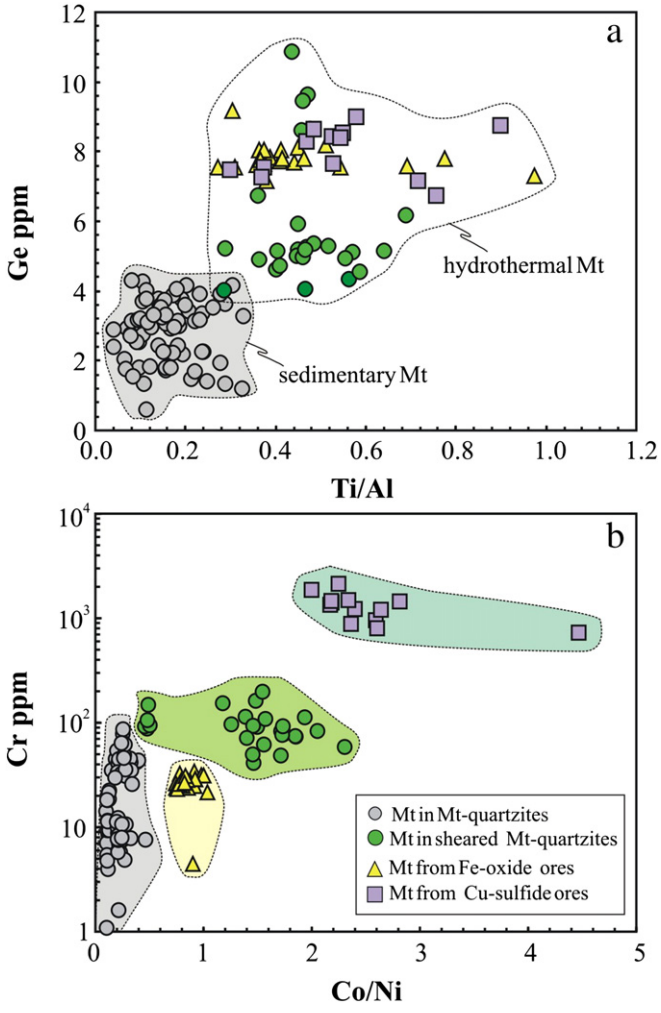

Fig. 8. Plots of Ga vs. Ti/Al (a) and Cr vs. Co/Ni (b) in magnetite from different hosting rocks and ores in the Khetri copper belt. Note that Ge and Ti/Al can sufficiently discriminate hydrothermal magnetite from BIF-type magnetite, while Cr and Co/Ni can clearly discriminate all the different types of magnetite in the copper belt.

combination of element pairs, Ge versus Ti/Al and Cr versus Co/Ni, can be used to discriminate BIF-type, sheared, and different hydrothermal magnetite in the Khetri belt. Our work agrees well with previous studies that composition of magnetite can be potentially very useful for discriminating different deposits, but also highlights that the discrimination schemes would be more meaningful for deposits from a certain region if fluid/water compositions and specific formation conditions reflected in composition of magnetite are clearly understood.

Conflict of interet

The authors declare that they have no conflict of interets.

Acknowledgments

This study is supported by the National Natural Science Foundation of China (41272212), the CAS/SAFEA International Partnership Program for Creative Research Teams-Intraplate Mineralization Research Team (KZZD-EW-TZ-20), and a CRCG grant (201309175142). We also appreciate the field assistance by Mr. A.K. Singh, Mr. V.N. Mishra and Mr. B. Patra from the Khetri Mine. Dr Guohui Hu and Dr. Yanyan Zhou are greatly appreciated for helping with analyses. Two anonymous reviewers and the guest editor, Prof. Rucheng Wang, provided useful suggestions for an earlier version of the manuscript and are gratefully acknowledged.

Appendix A. Supplementary data

Supplementary data to this article can be found online at http://dx.doi.org/10.1016/j.oregeorev.2014.09.035.

References

Bhattacharya, H.N., Bull, S., 2010. Tectono-sedimentary setting of the Paleoproterozoic Zawar Pb–Zn deposits, Rajasthan, India. Precambrian Res. 177, 323–338.
Biju-Sekhar, S., Yokoyama, K., Pandit, M.K., Okudaira, T., Yoshida, M., Santosh, M., 2003. Late Paleoproterozoic magmatism in Delhi Fold Belt, NW India and its implication: evidence from EPMA chemical ages of zircons. J. Asian Earth Sci. 22, 189–207.
Buddington, A.F., Lindsley, D.H., 1964. Iron-titanium oxide minerals and synthetic equivalents. J. Petrol. 5, 310–357.
Carew, M.J., 2004. Controls on Cu–Au Mineralization and Fe oxide Metasomatism in the Eastern Fold Belt, N.W. Queensland, Australia(Unpublished thesis) James Cook University.
Carranza, E.J.M., Rondeau, B., Cenki-Tok, B., Fritsch, E., Mazzero, F., Gauthier, J., Bodeur, Y., Bekele, E., Gaillou, E., Ayalew, D., 2012. Geochemical characteristics of mineral deposits: implications for ore genesis. Geochem. Explor. Environ. Anal. 12, 89.
Chaudhri, N., Kaur, P., Okrusch, M., Schimrosczyk, A., 2003. Characterisation of the Dabla granitoids, North Khetri Copper Belt, Rajasthan, India: evidence of bimodal anorogenic felsic magmatism. Gondwana Res. 6, 879–895.
Chung, D., Zhou, M.F., Gao, J.F., Chen, W.T., 2015. In-situ LA-ICP-MS trace elemental analyses of magnetite: the Paleoroterozoic Sokoman Iron Formation in the Labrador Trough, Canada. Ore Geol. Rev. 65, 917–928 (in this issue).
Dare, S.A.S., Barnes, S.-J., Beaudoin, G., 2012. Variation in trace element content of magnetite crystallized from a fractionating sulfide liquid, Sudbury, Canada: implications for provenance discrimination. Geochim. Cosmochim. Acta 88, 27–50.
Dare, S.A.S., Barnes, S.J., Beaudoin, G., Meric, J., Boutroy, E., Potvin-Doucet, C., 2014. Trace elements in magnetite as petrogenetic indicators. Mineral. Deposita http://dx.doi.org/10.1007/s00126-014-0529-0.
Das Gupta, S.P., 1968. The structural history of the Khetri Copper Belt, Jhunjhunu and Sikar districts, Rajasthan. Mem. Geol. Surv. India 98, 170.
Dupuis, C., Beaudoin, G., 2011. Discriminant diagrams for iron oxide trace element fingerprinting of mineral deposit types. Mineral. Deposita 46, 319–335.
Frietsch, R., Perdahl, J.A., 1995. Rare earth elements in apatite and magnetite in Kiruna-type iron ores and some other iron ore types. Ore Geol. Rev. 9, 489–510.
Frost, B., Lindsley, D.H., 1991. Occurrence of iron-titanium oxides in igneous rocks. Rev. Mineral. Geochem. 25, 433–468.
Gangopadhyay, P.K., Sen, R., 1967. On the occurrence of andalusite near Bairawas, Alwar Dist., Rajasthan. Quarterly Journal of Geological Min. Met. Society India 39, 39–41.
Gao, J.-F., Zhou, M.-F., Lightfoot, P.C., Wang, C.Y., Qi, L., Sun, M., 2013. Sulfide saturation and magma emplacement in the formation of the Permian Huangshandong Ni–Cu Sulfide Deposit, Xinjiang, Northwestern China. Econ. Geol. 108, 1833–1848.
Goldschmidt, V.M., 1958. Geochemistry. Oxford University Press, Amen House London.
Gopalan, K., Macdougall, J.D., Roy, A.B., Murli, A.V., 1990. Sm–Nd evidence for 3.3 Ga old rocks in Rajasthan, northwestern India. Precambrian Res. 48, 287–297.
Hou, K.J., Li, Y.H., Ye, T.R., 2009. In-situ U–Pb zircon dating laser ablation-multi iron counting-ICP-MS. Mineral Deposits 28, 481–492 (in Chinese with English abstract).
Hu, H., Li, J.W., Lentz, D., Ren, Z., Zhao, X.F., Deng, X.D., Hall, D., 2014. Dissolution–reprecipitation process of magnetite from the Chengchao iron deposit: insights into ore genesis and implication for in-situ chemical analysis of magnetite. Ore Geol. Rev. 57, 393–405.
Huang, X.W., Zhao, X.F., Qi, L., Zhou, M.F., 2013. Re–Os and S isotopic constraints on the origins of two mineralization events at the Tangdan sedimentary rock-hosted stratiform Cu-deposit, SW China. Chem. Geol. 347, 9–19.
Ilton, E.S., Eugster, H.P., 1989. Base metal exchange between magnetite and chloride-rich hydrothermal fluid. Geochem. Cosmichim. Acta 53, 291–301.
Jaireth, S., 1984. Ore paragenesis and fluid-inclusion thermometry of copper sulphide ores from Madhan-Kudhan and Kolihan deposits. Spec. Publ. Geol. Surv. India 12, 551–568.
Jaireth, S., 1986. Igneous source of sulfur of sulphides from Madhan-Kudhan and Kolihan deposits, Khetri copper belt, Rajasthan. J. Geol. Soc. India 27, 359–368.
Kaur, G., Mehta, P.K., 2005. The Gothara plagiogranite: evidence for oceanic magmatism in a non-ophiolitic association, North Khetri copper belt, Rajasthan, India? J. Asian Earth Sci. 25, 805–819.
Kaur, P., Chaudhri, N., Okrusch, M., Koepke, J., 2006. Palaeoproterozoic A-type felsic magmatism in the Khetri Copper Belt, Rajasthan, northwestern India: petrologic and tectonic implications. Mineral. Petrol. 87, 81–122.
Kaur, P., Chaudhri, N., Raczek, I., Kröner, A., Hofmann, A.W., 2007. Geochemistry, zircon ages and whole-rock Nd isotopic systematics for Palaeoproterozoic A-type granitoids in the northern part of the Delhi belt, Rajasthan, NW India: implications for late Palaeoproterozoic crustal evolution of the Aravalli craton. Geol. Mag. 144, 361–378.
Kaur, P., Chaudhri, N., Raczek, I., Kröner, A., Hofmann, A.W., 2009. Record of 1.82 Ga Andean-type continental arc magmatism in NE Rajasthan, India: insights from zircon and Sm–Nd ages, combined with Nd–Sr isotope geochemistry. Gondwana Res. 16, 56–71.
Kaur, P., Chaudhri, N., Raczek, I., Kröner, A., Hofmann, A.W., Okrusch, M., 2011. Zircon ages of late Palaeoproterozoic (ca. 1.72–1.70 Ga) extension-related granitoids in NE Rajasthan, India: regional and tectonic significance. Gondwana Res. 19, 1040–1053.
Klein, C., 2005. Some Precambrian banded iron-formations (BIFs) from around the world: their age, geologic setting, mineralogy, metamorphism, geochemistry, and origins. Am. Mineral. 90, 1473–1499.

Klemm, D.D., Henckel, J., Dehm, R.M., Von Gruenewaldt, G., 1985. The geochemistry of titanomagnetite in magnetite layers and their host rocks of the eastern Bushveld Complex. Econ. Geol. 80, 1075–1088.
Knight, J., Joy, S., Lowe, J., Cameron, J., Merrillees, J., Nag, S., Shah, N., Dua, G., Jhala, K., 2002. The Khetri copper belt, Rajasthan: iron-oxide copper-gold terrane in the Proterozoic of NW India. In: Porter, T.M. (Ed.), Hydrothermal Iron Oxide Copper-Gold & Related Deposits: a global perspective volume 2. PGC Publishing, Adelaide, pp. 321–341.
Lascelles, D.F., 2007. Black smokers and density currents: a uniformitarian model for genesis of banded iron-formations. Ore Geol. Rev. 32, 381–411.
Lister, G.F., 1966. The composition and origin of selected iron-titanium deposits. Econ. Geol. 61, 275–310.
Liu, Y.S., Hu, Z.C., Gao, S., Gunther, D., Xu, J., Gao, C.G., Chen, H.H., 2008. In situ analysis of major and trace elements of anhydrous minerals by LA-ICP-MS without applying an internal standard. Chem. Geol. 257, 34–43.
Liu, P.P., Zhou, M.F., Chen, W.T., Gao, J.F., Huang, X.W., 2015. In-situ LA-ICP-MS trace elemental analyses of magnetite: Fe-Ti-(V) oxide-bearing mafic-ultramafic layered intrusions of the Emeishan Large Igneous Province, SW China. Ore Geol. Rev. 65, 853–871 (in this issue).
Nadoll, P., Koenig, A.E., 2011. LA-ICP-MS of magnetite: methods and reference materials. J. Anal. At. Spectrom. 26, 1872–1877.
Nadoll, P., Mauk, J.L., Hayes, T.S., Koenig, A.E., Box, S.E., 2012. Geochemistry of magnetite from hydrothermal ore deposits and host rocks of the Mesoproterozoic Belt Supergroup, United States. Econ. Geol. 107, 1275–1292.
Nadoll, P., Angerer, T., Mauk, J.L., French, D., Walshe, J., 2014. The chemistry of hydrothermal magnetite: a review. Ore Geol. Rev. 61, 1–32.
Neilson, R., 2003. Trace element partitioning. http://earthref.org/GERM/tolls/tep.htm.
Nystrom, J.O., Henriquez, F., 1994. Magmatic features of iron ores of the Kiruna type in Chile and Sweden: ore textures and magnetite geochemistry. Econ. Geol. 89, 820–839.
Pearce, J.A., Gale, G., 1977. Identification of ore-deposition environment from trace-element geochemistry of associated igneous host rocks. Geol. Soc. Lond., Spec. Publ. 7, 14–24.
Rollinson, H., 1993. Using geochemical data. Longman, London, p. 352.
Roy, A.B., 2000. Geology of the Palaeoproterozoic Aravalli Supergroup of Rajasthan and northern Gujarat. In: Deb, M. (Ed.), Crustal Evolution and Metallogeny in the Northwestern Indian Shield. Narosa Publishing House, New Delhi, pp. 87–114.
Roy, A.B., Kröner, A., 1996. Single zircon evaporation ages constraining the growth of the Archaean Aravalli craton, northwestern Indian Shield. Geol. Mag. 133, 333–342.
Sarkar, S.C., Dasgupta, S., 1980. Geologic Setting, genesis and transformation of the sulfide deposits in the northern part of the Khetri copper belt, Rajasthan, India: an outline. Mineral. Deposita 15, 117–137.
Singh, S.P., 1988. Stratigraphy and sedimentation pattern in the Proterozoic Delhi Supergroup, Northwestern India. In: Roy, A.B. (Ed.), Precambrian of the Aravalli Mountain, Rajasthan, India. Mem. Geol. Soc. India vol. 7, pp. 193–205.
Singoyi, B., Danyushevsky, L., Davidson, G.J., Large, R., Zaw, K., 2006. Determination of trace elements in magnetites from hydrothermal deposits using the LA-ICP-MS technique. Abstracts of Oral and Poster Presentations from the SEG 2006 Conference Society of Economic Geologists, Keystone, USA, pp. 367–368.
Sinha-Roy, S., 1988. Proterozoic Wilson cycles in Rajasthan. In: Roy, A.B. (Ed.), Precambrian of the Aravalli Mountain, Rajasthan, India. Mem. Geol. Soc. India vol. 7, pp. 95–107.
Toplis, M.J., Carroll, M.R., 1995. An experimental study of the influence of oxygen fugacity on Fe–Ti oxide stability, phase relations, and mineral—melt equilibria in ferro-basaltic systems. J. Petrol. 36, 1137–1170.
Toplis, M.L., Corgne, A., 2002. An experimental study of element partitioning between magnetite, clinopyroxene and iron-bearing silicate liquids with particular emphasis on vanadium. Contrib. Mineral. Petrol. 144, 22–37.
Wager, L.R., Brown, G.M., 1968. Layered Igneous Rock. Oliver & Boyd, Edinburgh (588 pp.).
Wang, E.D., Xia, J.M., Fu, J.F., Jia, S.S., Men, Y.K., 2014. Formation mechanism of Gongchangling high-grade magnetite deposit hosted in Archean BIF, Anshan-Benxi area, Northeastern China. Ore Geol. Rev. 57, 308–321.
Wiedenbeck, M., Goswami, J.N., 1994. High-precision $^{207}Pb/^{206}Pb$ zircon geochronology using a small ion microprobe. Geochim. Cosmochim. Acta 58, 2135–2141.
Wiedenbeck, M., Goswami, J.N., Roy, A.B., 1996. Stabilization of the Aravalli craton of northwestern India at 2.5 Ga: an ion microprobe zircon study. Chem. Geol. 129, 325–340.
Zhao, W.W., Zhou, M.F., 2015. In-situ LA-ICP-MS trace elemental analyses of magnetite: the Mesozoic Tengtie skarn Fe deposit in the Nanling Range, South China. Ore Geol. Rev. 65, 872–883 (in this issue).
Zhou, M.-F., Robinson, P.T., Lesher, C.M., Keays, R.R., Zhang, C.J., Malpas, J., 2005. Geochemistry, petrogenesis and metallogenesis of the Panzhihua gabbroic layered intrusion and associated Fe–Ti–V oxide deposits, Sichuan Province, SW China. J. Petrol. 46, 2253–2280.
Zhou, M.-F., Chen, W.T., Wang, C.Y., Prevec, S.A., Liu, Patricia P., Howarth, G.H., 2013. Two stages of immiscible liquid separation in the formation of Panzhihua-type Fe–Ti–V oxide deposits, SW China. Geosci. Front. 4, 481–502.